

Cobalt(III) Alkyl Complexes of 1,2-Bis(2-pyridinecarboxamido)benzene (H_2bpb) and 4,5-Dichloro-1,2-bis(2-pyridinecarboxamido)benzene (H_2bpc) and X-Ray Crystal Structures of $[Co(bpc)(CH_2CH_2CMe=CH_2)(H_2O)]$ and $[Co(bpb)Et(H_2O)]^\ddagger$

Shing-Tat Mak, Wing-Tak Wong, Vivian Wing-Wah Yam, Ting-Fong Lai† and Chi-Ming Che*
Department of Chemistry, University of Hong Kong, Pokfulam Road, Hong Kong

A series of organo and non-organocobalt complexes of bpb and bpc ligands [H_2bpb = 1,2-bis(2-pyridinecarboxamido)benzene, H_2bpc = 4,5-dichloro-1,2-bis(2-pyridinecarboxamido)benzene] have been synthesised. Complexes prepared include $Na[CoL(CN)_2]$, $Na[CoL(N_3)_2]$, $[CoL(py)_2]ClO_4$ and $[CoL(R)(H_2O)]$ (L = bpb or bpc; py = pyridine; R = Me, Et, Prⁱ or $CH_2CH_2CMe=CH_2$). The complex $[CoL(CH_2CH_2CMe=CH_2)(H_2O)]$ was formed as a rearrangement product from the reaction of 3,3-dimethylallyl bromide and $[CoL]\cdot H_2O$ in the presence of $NaBH_4$ and $NaOH$ in methanol. The complexes $[Co(bpc)(CH_2CH_2CMe=CH_2)(H_2O)]$ **1** and $[Co(bpb)Et(H_2O)]$ **2** have been characterized by X-ray crystallography: **1**, space group $Pnma$, $a = 13.934(2)$, $b = 12.204(2)$, $c = 13.173(2)$ Å, $Z = 4$, and $R = 0.046$ for 1129 observed reflections; **2**, space group $Pnma$, $a = 15.072(1)$, $b = 12.119(2)$, $c = 9.884(3)$ Å, $Z = 4$, and $R = 0.034$ for 1387 observed reflections. Electrochemical studies on the one-electron oxidation of these complexes suggest the involvement of the equatorial ligand in these processes.

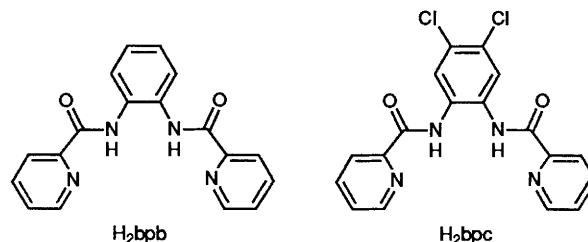
The importance of σ -organocobalt(III) complexes in vitamin B_{12} model studies is well documented.¹ With the exception of $[Co^{III}L^1(H_2O)]\cdot 2H_2O$ ² (L^1 = C⁷ radical of 1,5-diazacyclooctane-*N,N'*-diacetate) and $[CoL^2(R)(H_2O)]^{2+3}$ (L^2 = 1,4,8,11-tetraazacyclotetradecane), stable alkylcobalt(III) complexes are mainly confined to those species containing highly unsaturated ligands, such as porphyrins and Schiff bases. Recent studies on the co-ordination chemistry of the inexpensive dianionic organic amide ligands H_2bpb [1,2-bis(2-pyridinecarboxamido)benzene] and H_2bpc [4,5-dichloro-1,2-bis(2-pyridinecarboxamido)benzene] with manganese(III)⁴ and osmium(III)⁵ suggest that they exhibit oxidation chemistry similar to the corresponding metalloporphyrins and Schiff-base metal complexes. Thus, the use of these ligands to generate stable alkylcobalt(III) complexes seems attractive. Herein are described the synthesis and characterization of a series of cobalt(III) complexes of bpb and bpc ligands, and the X-ray crystal structures of $[Co(bpc)(CH_2CH_2CMe=CH_2)(H_2O)]$ and $[Co(bpb)Et(H_2O)]$.

Experimental

1,2-Phenylenediamine was recrystallized from hot ethanol before use. All solvents and chemicals used in syntheses were of reagent grade, and were used without further purification.

For electrochemical work, acetonitrile (Mallinckrodt, ChromAR) was distilled from CaH_2 before use. Methanol (Merck, extra pure) was dried by distillation over magnesium. Tetrabutylammonium tetrafluoroborate (Southwestern Analytical Chemicals, Electrometric grade) was dried at 100 °C under vacuum for 24 h before use.

All solutions for electrochemical studies were deaerated with prepurified argon gas. For electrochemical studies in non-aqueous medium, the argon gas was dried by passing through



sodium hydroxide, then activated molecular sieve (5 Å), and finally presaturated with the solvent used in the electrochemical studies before passing into the electrochemical cell.

Ligand Syntheses.—1,2-Bis(2-pyridinecarboxamido)benzene (H_2bpb) was synthesised by condensation of 1,2-phenylenediamine and pyridine-2-carboxylic acid in pyridine in the presence of triphenyl phosphite.⁶ Similarly, 4,5-dichloro-1,2-bis(2-pyridinecarboxamido)benzene (H_2bpc) was synthesised from 4,5-dichloro-1,2-phenylenediamine and pyridine-2-carboxylic acid.

Syntheses of Cobalt Complexes.— $[Co(bpb)]\cdot H_2O$. The complex was prepared according to the published procedure⁷ with slight modification. Cobalt(II) acetate tetrahydrate (1.0 g) was added to an aqueous suspension of H_2bpb (1.0 g, in 60 cm³) under a nitrogen atmosphere. The reaction mixture was heated to 90 °C and vigorously stirred for 1.5 h. The resulting brown precipitate was collected by suction filtration and washed successively with water and chloroform. The $[Co(bpb)]\cdot H_2O$ prepared was used without further purification for subsequent syntheses.

$[Co(bpc)]\cdot H_2O$. This was prepared similarly to $[Co(bpb)]\cdot H_2O$ with H_2bpc (1.0 g) used in place of H_2bpb , and the reaction mixture was heated and stirred for 3 instead of 1.5 h. The orange product $[Co(bpc)]\cdot H_2O$ was collected by filtration and washed with water. It was also used without further purification in subsequent syntheses.

† For correspondence on X-ray crystal structures.

‡ Supplementary data available: see Instructions for Authors, *J. Chem. Soc., Dalton Trans.*, 1991, Issue 1, pp. xviii–xxii.

$\text{Na}[\text{Co}(\text{bpb})(\text{CN})_2]$. Sodium cyanide (0.1 g) in methanol (5 cm^3) was added dropwise to a warm methanolic solution of $[\text{Co}(\text{bpb})\cdot\text{H}_2\text{O}]$ (0.2 g). After cooling to 0 °C, dichloromethane was added to the resulting red solution to precipitate the excess of NaCN. This was filtered off, and the filtrate was evaporated under vacuum to produce shiny red crystals of $\text{Na}[\text{Co}(\text{bpb})(\text{CN})_2]$. The crude product was obtained as dark red crystals by recrystallization from methanol–diethyl ether. Yield 70% {Found: C, 53.20; H, 2.90; N, 18.95. Calc. for $\text{Na}[\text{Co}(\text{bpb})(\text{CN})_2]$: C, 53.35; H, 2.70; N, 18.65%}. IR (Nujol mull): $\nu(\text{C}\equiv\text{N})$ 2100 cm^{-1} .

$\text{Na}[\text{Co}(\text{bpb})(\text{N}_3)_2]$. The complex $[\text{Co}(\text{bpb})\cdot\text{H}_2\text{O}]$ (0.2 g) was added to a suspension of NaN_3 (0.3 g) in acetone–water (10:1 v/v, 50 cm^3) to give a brown solution. This was refluxed for 2 h, and the mixture evaporated to dryness under reduced pressure. The residue was dissolved in acetone and the excess of NaN_3 was filtered off. Dark brown crystals of $\text{Na}[\text{Co}(\text{bpb})(\text{N}_3)_2]$ were obtained by diffusion of diethyl ether into the filtrate. Yield 60% {Found: C, 43.40; H, 3.45; N, 26.70. Calc. for $\text{Na}[\text{Co}(\text{bpb})(\text{N}_3)_2]\cdot\text{MeOH}\cdot 0.5\text{H}_2\text{O}$: C, 43.60; H, 3.25; N, 26.75%}. IR (Nujol mull): $\nu_{\text{asym}}(\text{N}\equiv\text{N})$ 2000 cm^{-1} .

$[\text{Co}(\text{bpb})(\text{py})_2]\text{ClO}_4$. Cobalt acetate tetrahydrate (1 mmol) was added to a refluxing mixture of pyridine (py) (1 cm^3) and H_2bpb (1 mmol) in methanol (50 cm^3) under a nitrogen atmosphere. The mixture was refluxed for an additional 1.5 h to give a reddish brown solution, which turned green immediately upon introduction of air. The solution was evaporated to dryness under vacuum. The residue was washed several times with diethyl ether and then dissolved in methanol. Lithium perchlorate was added and the solution was reduced in volume under reduced pressure to give green crystals of $[\text{Co}(\text{bpb})(\text{py})_2]\text{ClO}_4$. Green needle-shaped crystals were obtained by recrystallization from acetonitrile–diethyl ether. Yield 50% {Found: C, 52.85; H, 3.60; Cl, 5.8; N, 13.10. Calc. for $[\text{Co}(\text{bpb})(\text{py})_2]\text{ClO}_4$: C, 53.15; H, 3.50; Cl, 5.6; N, 13.30%}.

$[\text{Co}(\text{bpb})\text{R}(\text{H}_2\text{O})]$ (R = Me, Et, Prⁱ or $\text{CH}_2\text{CH}_2\text{CMe}=\text{CH}_2$). Sodium tetrahydroborate (30 mg) was added to a methanolic solution (40 cm^3) of $[\text{Co}(\text{bpb})\cdot\text{H}_2\text{O}]$ (150 mg) and NaOH (0.1 g) at room temperature under a nitrogen atmosphere. The mixture was stirred for 0.5 h during which the solution darkened and gave a dark green precipitate. Alkyl halide (0.5 cm^3 ; methyl iodide, ethyl iodide, isopropyl iodide or 3,3-dimethylallyl bromide, respectively) was added and stirred for 15 min. The resulting deep red solution was then reduced in volume under vacuum and water was added to precipitate the orange product. The crude product was chromatographed on an alumina (activity II) column using acetonitrile as eluent, and recrystallized from acetonitrile–diethyl ether: $[\text{Co}(\text{bpb})\text{Me}(\text{H}_2\text{O})]$, red powder, yield 75% {Found: C, 57.35; H, 4.60; N, 13.95. Calc. for $[\text{Co}(\text{bpb})\text{Me}(\text{H}_2\text{O})]$: C, 57.15; H, 4.05; N, 14.05%}; $[\text{Co}(\text{bpb})\text{Et}(\text{H}_2\text{O})]$, dark red crystals, yield 75% {Found: C, 57.00; H, 4.50; N, 13.35. Calc. for $[\text{Co}(\text{bpb})\text{Et}(\text{H}_2\text{O})]$: C, 56.90; H, 4.55; N, 13.25%}; $[\text{Co}(\text{bpb})\text{Pr}^i(\text{H}_2\text{O})]$, red powder, yield 70% {Found: C, 56.35; H, 4.75; N, 12.65. Calc. for $[\text{Co}(\text{bpb})\text{Pr}^i(\text{H}_2\text{O})]$: C, 56.40; H, 5.40; N, 12.50%}; $[\text{Co}(\text{bpb})(\text{CH}_2\text{CH}_2\text{CMe}=\text{CH}_2)(\text{H}_2\text{O})]$, orange needle-shaped crystals, yield 65% {Found: C, 58.55; H, 4.95; N, 12.20. Calc. for $[\text{Co}(\text{bpb})(\text{CH}_2\text{CH}_2\text{CMe}=\text{CH}_2)\cdot 1.5\text{H}_2\text{O}$: C, 58.60; H, 5.15; N, 11.90%}.

$\text{Na}[\text{Co}(\text{bpc})(\text{CN})_2]$. A methanolic solution (0.1 mol dm^{-3}) of NaCN was added dropwise to a suspension of $[\text{Co}(\text{bpc})\cdot\text{H}_2\text{O}]$ (0.2 g) in methanol at ca. 50 °C. The resulting orange solution was filtered and reduced in volume under vacuum to give an orange precipitate of $\text{Na}[\text{Co}(\text{bpc})(\text{CN})_2]$, which was recrystallized from acetone–diethyl ether to give orange needle-shaped crystals. Yield 75% {Found: C, 42.25; H, 2.35; Cl, 12.20; N, 15.10. Calc. for $\text{Na}[\text{Co}(\text{bpc})(\text{CN})_2]\cdot 2.5\text{H}_2\text{O}$: C, 42.60; H, 2.70; Cl, 12.55; N, 14.90%}. IR (Nujol mull): $\nu(\text{C}\equiv\text{N})$ 2100 cm^{-1} .

$\text{Na}[\text{Co}(\text{bpc})(\text{N}_3)_2]$. The complex $[\text{Co}(\text{bpc})\cdot\text{H}_2\text{O}]$ (0.2 g) was added to a suspension of sodium azide (0.3 g) in acetone–water (10:1 v/v, 50 cm^3) and refluxed for 2.5 h. The mixture was

evaporated to dryness and then dissolved in acetone. Excess of NaN_3 was removed by filtration and diethyl ether was allowed to diffuse into the filtrate to give brown crystals of $\text{Na}[\text{Co}(\text{bpc})(\text{N}_3)_2]$. Yield 50% {Found: C, 37.60; H, 2.50; Cl, 11.55; N, 23.85. Calc. for $\text{Na}[\text{Co}(\text{bpc})(\text{N}_3)_2]\cdot 1.5\text{H}_2\text{O}$: C, 37.35; H, 2.25; Cl, 12.25; N, 24.20%}. IR (Nujol mull): $\nu_{\text{asym}}(\text{N}_3)$ 2000 cm^{-1} .

$[\text{Co}(\text{bpc})(\text{py})_2]\text{ClO}_4$. Cobalt(II) acetate tetrahydrate (1 mmol) was added to a methanolic suspension (50 cm^3) of H_2bpc (1 mmol) and pyridine (1 cm^3) under a nitrogen atmosphere. After refluxing for 0.5 h, air was introduced into the resulting orange suspension which gradually turned green. Lithium perchlorate was added to a methanolic solution of the product, and the volume reduced under vacuum. Pure green solid $[\text{Co}(\text{bpc})(\text{py})_2]\text{ClO}_4$ was obtained by recrystallization from hot acetonitrile {Found: C, 48.15; H, 2.65; Cl, 15.15; N, 12.15. Calc. for $[\text{Co}(\text{bpc})(\text{py})_2]\text{ClO}_4$: C, 47.90; H, 2.85; Cl, 15.15; N, 11.95%}.

$[\text{Co}(\text{bpc})\text{R}(\text{H}_2\text{O})]$ (R = Me, Et or $\text{CH}_2\text{CH}_2\text{CMe}=\text{CH}_2$). Sodium tetrahydroborate (30 mg) was added to a suspension of $[\text{Co}(\text{bpc})\cdot\text{H}_2\text{O}]$ (150 mg) and NaOH (0.1 g) in methanol (40 cm^3) at 50 °C under nitrogen, and was stirred for 45 min. The resulting dark green suspension was then cooled to 0 °C and alkyl halide (0.5 cm^3 ; methyl iodide, ethyl iodide or 3,3-dimethylallyl bromide, respectively) was added, and was stirred for an additional 15 min. The deep red solution obtained was filtered, reduced in volume, and the orange product precipitated by addition of water. Recrystallization was carried out in methanolic solution by slow evaporation: $[\text{Co}(\text{bpc})\text{Me}(\text{H}_2\text{O})]$, yield 70% {Found: C, 47.05; H, 3.50; Cl, 13.90; N, 11.55. Calc. for $[\text{Co}(\text{bpc})\text{Me}(\text{H}_2\text{O})]\cdot 1.5\text{H}_2\text{O}$: C, 46.95; H, 3.30; Cl, 14.60; N, 11.50%}; $[\text{Co}(\text{bpc})\text{Et}(\text{H}_2\text{O})]$, yield 70% {Found: C, 50.55; H, 3.55; Cl, 14.20; N, 11.65. Calc. for $[\text{Co}(\text{bpc})\text{Et}(\text{H}_2\text{O})]$: C, 50.75; H, 3.20; Cl, 14.60; N, 11.85%}; $[\text{Co}(\text{bpc})(\text{CH}_2\text{CH}_2\text{CMe}=\text{CH}_2)(\text{H}_2\text{O})]$, yield 60%.

Physical Measurements and Instrumentation.—Infrared spectra were obtained as Nujol mulls on a Perkin-Elmer model 577 spectrophotometer, ultraviolet–visible spectra on a Shimadzu UV-240 spectrophotometer, and NMR spectra on a JEOL model FX90Q spectrometer (90 MHz). Chemical shifts are reported relative to tetramethylsilane as standard. Elemental analyses were performed by the Microanalytical unit of the Australian Mineral Development Laboratories.

Cyclic voltammetric measurements were carried out using a Princeton Applied Research (PAR) model 175 universal programmer, model 173 potentiostat and model 179 digital coulometer coupled to a Houston 2000 X-Y recorder. A conventional two-compartment cell was used as the electrolytic cell. The salt bridge of the reference electrode was separated from the working electrode compartment by a Vycor glass. A platinum foil was used as the counter electrode. In aqueous media a saturated calomel electrode (SCE) was used as the reference electrode. In non-aqueous media a Ag–AgNO₃ (0.1 mol dm^{-3} in MeCN) reference electrode was used, with the ferrocenium–ferrocene couple as the internal standard. The working electrodes used were either glassy carbon (Atomergic Chemetals V25) or platinum (Beckman Instruments). Controlled-potential coulometry was performed using a PAR model 173 potentiostat and the quantity of electricity passed was measured by a PAR model 179 digital coulometer. The working electrode was a glassy carbon crucible (Atomergic Chemetals V25-12). During controlled-potential electrolysis the electrolyte was stirred with a synchronous stirring motor and purged with purified argon. Ultraviolet–visible spectral changes were monitored by withdrawing aliquots of sample solution from the electrolytic cell during electrolysis.

Rotating-disc voltammetry was performed using a Pine Instrument model RDE4 bipotentiostat with a ASR-2 analytical rotator. The electrodes were treated as in cyclic voltammetry.⁸

X-Ray Structure Determination of $[\text{Co}(\text{bpc})(\text{CH}_2\text{CH}_2\text{CMe}=\text{CH}_2)(\text{H}_2\text{O})]$

Table 1 Fractional atomic coordinates for non-hydrogen atoms in [Co(bpc)(CH₂CH₂CMe=CH₂)(H₂O)] with estimated standard deviations (e.s.d.s) in parentheses

Atom	x	y	z
Co	0.491 19(6)	0.250	0.353 89(7)
Cl	0.099 9(1)	0.378 7(2)	0.629 9(1)
O(1)	0.381 2(2)	0.538 7(3)	0.434 7(2)
O(2)	0.577 8(3)	0.250	0.487 7(4)
N(1)	0.408 6(2)	0.353 7(3)	0.412 5(3)
N(2)	0.561 0(3)	0.381 8(3)	0.309 3(3)
C(1)	0.187 3(3)	0.305 3(4)	0.563 0(3)
C(2)	0.258 0(3)	0.364 4(5)	0.513 6(4)
C(3)	0.330 4(3)	0.306 9(4)	0.463 7(3)
C(4)	0.427 5(3)	0.459 1(4)	0.401 8(3)
C(5)	0.517 5(3)	0.474 9(4)	0.340 9(3)
C(6)	0.553 0(4)	0.577 9(4)	0.319 6(4)
C(7)	0.636 8(4)	0.587 1(4)	0.264 0(4)
C(8)	0.680 9(3)	0.494 3(4)	0.233 0(4)
C(9)	0.642 3(3)	0.393 6(4)	0.255 7(4)
C(10)	0.410 8(5)	0.250	0.228 7(5)
C(11)	0.456 7(6)	0.250	0.127 9(6)
C(12)	0.383 0(6)	0.250	0.042 5(6)
C(13)	0.330 7(9)	0.334(1)	0.007(1)
C(14)	0.362(1)	0.133(1)	0.012(1)

Table 2 Fractional atomic coordinates for non-hydrogen atoms in [Co(bpb)Et(H₂O)] with e.s.d.s in parentheses

Atom	x	y	z
Co	0.541 58(3)	0.250	0.319 59(5)
O(1)	0.624 7(1)	0.542 0(1)	0.458 2(2)
O(2)	0.438 5(2)	0.250	0.468 0(3)
N(1)	0.605 6(1)	0.354 2(2)	0.420 3(2)
N(2)	0.486 4(1)	0.383 2(2)	0.240 9(2)
C(1)	0.775 9(2)	0.306 9(3)	0.689 9(3)
C(2)	0.721 4(2)	0.366 0(2)	0.601 5(3)
C(3)	0.666 5(2)	0.307 8(2)	0.512 5(2)
C(4)	0.589 9(2)	0.461 4(2)	0.401 2(2)
C(5)	0.519 7(2)	0.476 5(2)	0.295 3(2)
C(6)	0.490 6(2)	0.580 0(2)	0.256 9(3)
C(7)	0.424 5(2)	0.588 3(3)	0.160 9(3)
C(8)	0.391 0(3)	0.494 4(3)	0.105 8(4)
C(9)	0.422 5(2)	0.394 4(3)	0.148 8(3)
C(10)	0.627 2(3)	0.250	0.168 0(4)
C(11)	0.707 1(5)	0.315 3(6)	0.167 2(7)

CH₂(H₂O)].—*Crystal data.* C₂₃H₂₁Cl₂CoN₄O₃, *M* = 531.28, orthorhombic, space group *Pnma*, *a* = 13.934(2), *b* = 12.204(2), *c* = 13.173(2) Å, *U* = 2240(1) Å³, *D_m* = 1.53 g cm⁻³, *Z* = 4, *D_c* = 1.575 g cm⁻³, *F*(000) = 1088, μ(Mo-Kα, λ = 0.710 73 Å) = 10.3 cm⁻¹. Crystal dimensions: 0.11 × 0.16 × 0.17 mm. Intensities (2 < 2θ < 50°; *h, k, ±l*; ω-2θ scan at 1.1–5.5° min⁻¹) were measured at 25 °C on an Enraf-Nonius CAD4 diffractometer and corrected for Lorentz and polarization effects but no absorption correction was made. A total of 4336 reflections were measured, of which 2266 were unique and 1129 [*F_o* > 2σ(*F_o*)] were considered observed.

The structure was solved by direct methods with MULTAN 82⁹ and refined by full-matrix least squares. The two disordered carbon atoms of the 3-methylbutenyl group were refined isotropically and the rest of the non-hydrogen atoms anisotropically. The hydrogen atoms of the water molecule were located from a Fourier difference map and all other hydrogen atoms were generated geometrically (C–H 0.95 Å) with assigned isotropic thermal parameters; all hydrogen parameters were not refined. Systematic absences suggested that space group to be *Pnma* or *Pn2₁a* and proved to be *Pnma* by the convergence of refinement. The function minimized was Σw(|*F_o*| – |*F_c*|)² with weighting scheme *w* = 4*F_o*²/[σ²(*F_o*²) + (*pF_o*²)²], *p* = 0.04. The final *R* values are: *R* = 0.046, *R'* = 0.044, goodness of fit = 1.087. The shift (Δ/σ) in the final cycle was less than 0.13σ. The

final Fourier difference map showed no significant features (ρ_{max} = 0.4 e Å⁻³). Atomic coordinates of non-hydrogen atoms are given in Table 1.

X-Ray Structure Determination of [Co(bpb)Et(H₂O)].—Crystal data. C₂₀H₁₉CoN₄O₃, *M* = 422.33, orthorhombic, space group *Pnma*, *a* = 15.072(1), *b* = 12.119(2), *c* = 9.884(3) Å, *U* = 1805.4 Å³, *D_m* = 1.55 g cm⁻³, *Z* = 4, *D_c* = 1.553 g cm⁻³, *F*(000) = 872, μ(Mo-Kα, λ = 0.710 73 Å) = 9.8 cm⁻¹. Crystal dimensions: 0.05 × 0.30 × 0.35 mm. Intensities (2 < 2θ < 52°; *h, k, ±l*; ω-2θ scan at 0.92–5.5° min⁻¹) were measured at 25 °C on an Enraf-Nonius CAD4 diffractometer and corrected for Lorentz and polarization effects, but not for absorption. A total of 3936 reflections were measured, of which 2049 were unique and 1387 [*F_o* > 3σ(*F_o*)] considered observed.

The structure was solved by the heavy-atom method and refined by full-matrix least squares. The disordered methyl carbon atom was refined isotropically and the rest of the non-hydrogen atoms anisotropically. Hydrogen atoms of the water molecule were located from a Fourier difference synthesis while other hydrogen atoms were generated geometrically; all the hydrogen atoms with assigned isotropic thermal parameters were not refined. The refinement converged to *R* = 0.034, *R'* = 0.043 and goodness of fit = 1.341. The parameter shifts in the last cycle were less than 0.09σ. The final Fourier difference map was featureless and the residual electron density was in the range of –0.27 to 0.59 e Å⁻³. Atomic coordinates of non-hydrogen atoms are given in Table 2. Computations were carried out on a MicroVax II computer using the SDP programs.¹⁰ The atomic scattering factors were taken from ref. 11.

Additional material available from the Cambridge Crystallographic Data Centre comprises H-atom coordinates, thermal parameters, and remaining bond angles.

Results and Discussion

The complexes [Co(bpb)]·H₂O and [Co(bpc)]·H₂O were prepared by a modified procedure of Chapman and Vagg,⁷ which involved the addition of cobalt(II) acetate to an aqueous suspension of the ligand under a nitrogen atmosphere. Instead of obtaining a mixture of products as reported previously, each complex was isolated as the sole product. Reaction of [Co(bpb)]·H₂O with sodium azide, sodium cyanide and pyridine gave the respective disubstituted cobalt(III) complexes, namely [Co(bpb)(N₃)₂]⁻, [Co(bpb)(CN)₂]⁻ and [Co(bpb)(py)₂]⁺. The identity of these complexes was confirmed by elemental analyses, IR spectroscopy and magnetic susceptibility measurements. The IR spectrum of [Co(bpb)(N₃)₂]⁻ shows a ν_{asym}(N≡N) stretch of 2000 cm⁻¹, typical of co-ordinated azide.¹² The ν(C≡N) stretch at 2100 cm⁻¹ of [Co(bpb)(CN)₂]⁻ is indicative of terminal cyanide group.¹² Magnetic susceptibility measurements show that all three complexes are diamagnetic, in accord with a low-spin (t_{2g})⁶ electronic configuration. Similar results were obtained with the Co(bpc) complexes.

In this work, Co–C bonds were formed by the reaction of Co^I with electrophilic reagents such as alkyl halide and olefins. Sodium tetrahydroborate was used as the reducing agent to generate Co^I from the corresponding [Co^{II}(bpb)]·H₂O and [Co^{II}(bpc)]·H₂O complexes under a nitrogen atmosphere and in the presence of sodium hydroxide. During reduction a dark green precipitate was obtained, typical of cobalt(I) complexes of ligands such as oximes, Schiff bases, corrinoids and porphyrins.¹³ This reacted rapidly with alkyl halides to give the desired red organocobalt(III) complexes.

Interestingly, addition of 3,3-dimethylallyl bromide to the cobalt(I) complexes did not generate the σ-allyl complex. Instead, the complex with the bpc ligand assumes the structure shown in Fig. 1. This has been confirmed by X-ray

Table 3 Proton NMR spectral data of some organocobalt(III) complexes [CoL(R)(H₂O)] (L = bpb or bpc) in CD₃OD*

bpb R' = H
bpc R' = Cl

Complex	bpb				Axial ligand
	H _β	H _α	H ⁶	H ³⁻⁵	
Me	6.99 (dd, 2 H, J _m = 3.50, J _o = 6.13)	8.60 (dd, 2 H, J _m = 3.50, J _o = 6.13)	9.00 [d, 2 H, J(H ⁵ H ⁶) = 5.25]	7.6–8.3 (m, 6 H)	1.65 (s, 3 H, CH ₃)
Et	6.96 (dd, 2 H, J _m = 3.50, J _o = 6.13)	8.58 (dd, 2 H, J _m = 3.50, J _o = 6.12)	8.97 [d, 2 H, J(H ⁵ H ⁶) = 5.25]	7.6–8.3 (m, 6 H)	2.73 (q, 2 H, J = 7.5, CH ₂) 0.13 (t, 3 H, J = 7.5, CH ₃)
Pr ⁱ	6.97 (dd, 2 H, J _m = 3.50, J _o = 6.13)	8.58 (dd, 2 H, J _m = 3.50, J _o = 6.13)	9.02 [d, 2 H, J(H ⁵ H ⁶) = 5.25]	7.6–8.3 (m, 6 H)	–0.13 (d, 6 H, J = 7.0, CH ₃)
CH ^a ₂ CH ^b ₂ C(CH ^c ₃)=CH ^d H	6.98 (dd, 2 H, J _m = 3.50, J _o = 6.13)	8.60 (dd, 2 H, J _m = 3.50, J _o = 6.13)	9.01 [d, 2 H, J(H ⁵ H ⁶) = 5.25]	7.6–8.3 (m, 6 H)	2.67 [t, 2 H, J(H ^a H ^b) = 8.31, H ^a] 1.28 [t, 2 H, J(H ^a H ^b) = 8.31, H ^b] 4.29, 4.35 (2 H, H ^c , H ^d) 1.37 (s, 3 H, H ^e)
bpc					
	H _α	H ⁶	H ³⁻⁵		
Me	8.70 (s, 2 H)	8.99 [d, 2 H, J(H ⁵ H ⁶) = 5.25]	7.6–8.4 (m, 6 H)		1.73 (s, 3 H, CH ₃)
Et	8.69 (s, 2 H)	8.98 [d, 2 H, J(H ⁵ H ⁶) = 6.12]	7.6–8.5 (m, 6 H)		2.81 (q, 2 H, J = 7.5, CH ₂) 1.18 (t, 3 H, J = 7.5, CH ₃)
CH ^a ₂ CH ^b ₂ C(CH ^c ₃)=CH ^d H	8.70 (s, 2 H)	9.00 [d, 2 H, J(H ⁵ H ⁶) = 6.12]	7.6–8.4 (m, 6 H)		2.73 [t, 2 H, J(H ^a H ^b) = 7.44, H ^a] 1.17 [t, 2 H, J(H ^a H ^b) = 7.43, H ^b] 4.32, 4.38 (2 H, H ^c , H ^d) 1.40 (s, 3 H, H ^e)

* Chemical shifts δ are with reference to SiMe₄ in CD₃OD solution, coupling constants, J , in Hz.

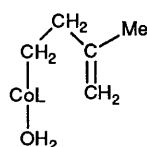
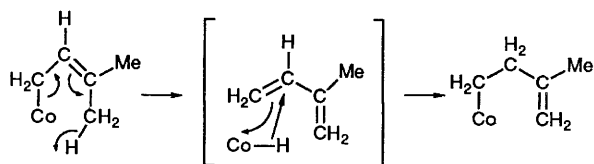


Fig. 1 Structure of the product formed from the reaction between 3,3-dimethylallyl bromide and [Co(bpc)]·H₂O in the presence of NaBH₄ in methanol



Scheme 1

crystallography. The isolation of [Co(bpc)(CH₂CH₂CMe=CH₂)(H₂O)] in the reaction between [Co(bpc)][−] and Me₂C=CHCH₂Br is rather intriguing since [Co^{III}(bpc)-(CH₂CH=CMe₂)] is the expected oxidative-addition product. It is likely that [Co^{III}(bpc)(CH₂CH=CMe₂)] was initially formed but subsequently reacted through the pathway in Scheme 1. Such

intramolecular rearrangement of Me₂C=CHCH₂ to CH₂=CMe-CH₂ has not been reported previously.

The newly prepared metal complexes are all air-stable solids and have satisfactory elemental analyses. Their IR spectra all show a ν (C=O) stretch at 1610–1635 cm^{−1}, which is at a lower frequency than that of the free ligand [ν (C=O), H₂bpb, 1675 and 1665; H₂bpc, 1710 and 1693 cm^{−1}]. This together with the absence of ν (N–H) stretches indicates that the two co-ordinated amide groups are deprotonated.

The ¹H NMR spectral data of the organocobalt complexes are summarized in Table 3. The reasonably sharp NMR peaks were indicative of diamagnetic organocobalt derivatives. With the exception of the pyridyl protons which are complicated by long-range coupling effects, the assignments of the spectra are quite straightforward. The broad doublet at *ca.* δ 9 is assigned to the proton *ortho* to the N atom on the pyridine ring. The broadness probably is a result of its proximity to nitrogen which had a quadrupole moment.

Substitution of hydrogens at the β positions of the benzene bridge by chloro groups simplifies the interpretation of the spectra. The presence of only a singlet in the low-field region of the bpc complexes instead of two double doublets for the bpb complexes suggests that the signals in the low-field region are derived from the protons at the α positions, while those at high field are derived from the β -protons of the benzene bridge. Fig. 2

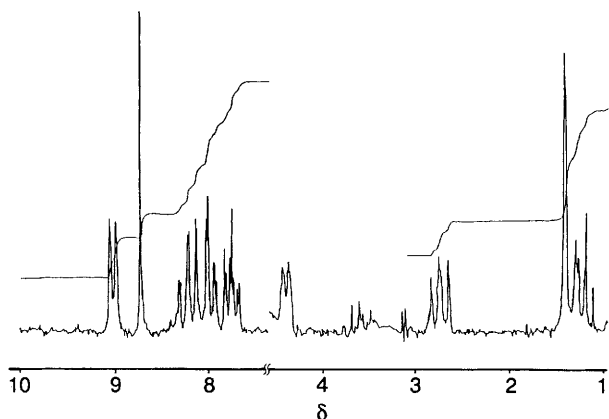


Fig. 2 Proton NMR spectrum of $[\text{Co}(\text{bpc})(\text{CH}_2\text{CH}_2\text{CMe}=\text{CH}_2)(\text{H}_2\text{O})]$ in CD_3OD

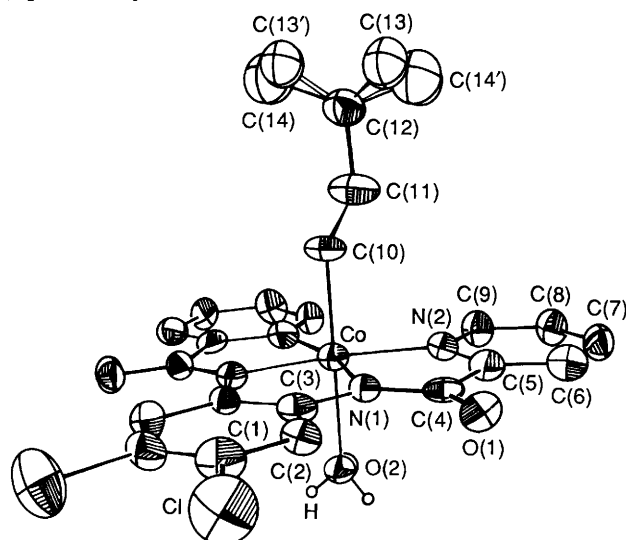


Fig. 3 ORTEP drawing of compound 1. Thermal ellipsoids are at the 30% probability level

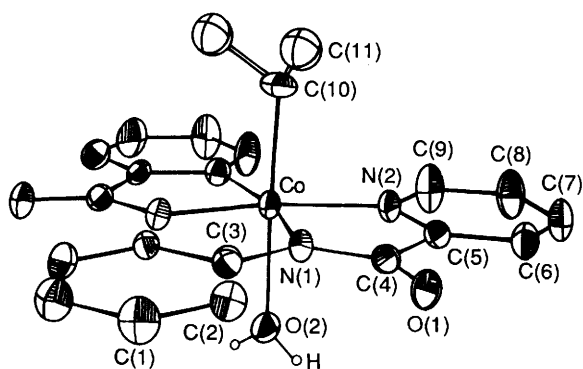


Fig. 4 ORTEP drawing of compound 2. Thermal ellipsoids are at the 30% probability level

shows the ^1H NMR spectrum of $[\text{Co}^{\text{III}}(\text{bpc})(\text{CH}_2\text{CH}_2\text{CMe}=\text{CH}_2)(\text{H}_2\text{O})]$; the signals at δ 4.38 and 4.32 are assigned to the geminal protons ($=\text{CH}_2$) with a coupling constant of *ca.* 6 Hz.

X-Ray Crystal Structures.—Not many cobalt(III) amide complexes have been reported in the literature.¹⁴ To our knowledge, these two structures constitute the first example of σ -alkylcobalt(III) complexes bearing an organic amide ligand. Figs. 3 and 4 show ORTEP drawings of $[\text{Co}(\text{bpc})(\text{CH}_2\text{CH}_2\text{CMe}=\text{CH}_2)(\text{H}_2\text{O})]$ **1** and $[\text{Co}(\text{bpb})\text{Et}(\text{H}_2\text{O})]$ **2** together with the atomic numbering schemes. The cobalt atom in both **1** and **2** is six-co-ordinated with a distorted-octahedral geometry. The

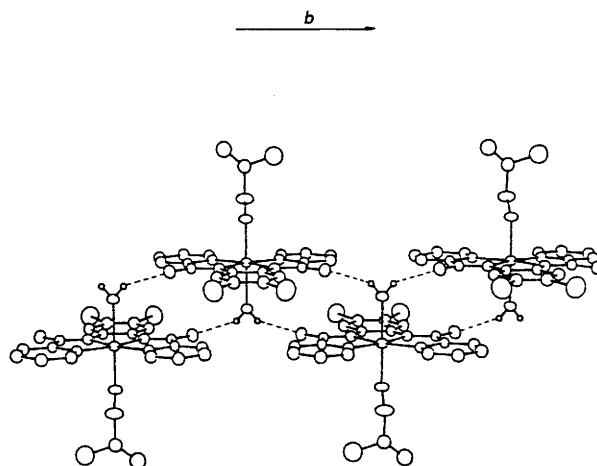


Fig. 5 Hydrogen-bonding scheme in compound 1

four nitrogen atoms in the amide ligand occupy the four equatorial positions and the cobalt atom together with the axial ligands are on the crystallographic mirror plane which bisects the amide ligand so that half a molecule constitutes an asymmetric unit.

Table 4 gives selected bond distances and angles for both complexes **1** and **2**. The values are very similar in the two structures. In **1** the 3-methylbutenyl group has a disordered structure with C(10), C(11) and C(12) on the crystallographic mirror plane and the disordered atoms C(13), C(13'), C(14) and C(14') out-of-plane. In accord with the ^1H NMR spectral data (Table 3), the co-ordinated alkyl group has a terminal C=C double bond [C(12)–C(13) 1.34(1) Å] which is necessarily shorter than C–C single bonds such as C(12)–C(11) [1.52(1) Å] and C(12)–C(14) [1.52(2) Å]. The Co–C bond length of 1.994(7) Å is in the usual range (1.98–2.01 Å) found in other σ -alkylcobalt(III) complexes having water *trans* to the alkyl group.^{3,15} The Co–N(amide) bond of 1.877(4) Å is longer than that in the analogous complex $\text{Na}[\text{Co}(\eta^4\text{-bhp})]\cdot\text{Me}_2\text{CO}$ [1.818(9) Å]^{14b} [H_4bhp = 1,2-bis(2-hydroxy-2-methylpropanamido)benzene] but shorter than the Co–N(pyridine) bond [1.970(4) Å]. The structural parameters of the bpc ligand are similar to the bpb ligand found in $[\text{Os}^{\text{III}}(\text{bpb})(\text{PPh}_3)\text{Cl}]$.⁵

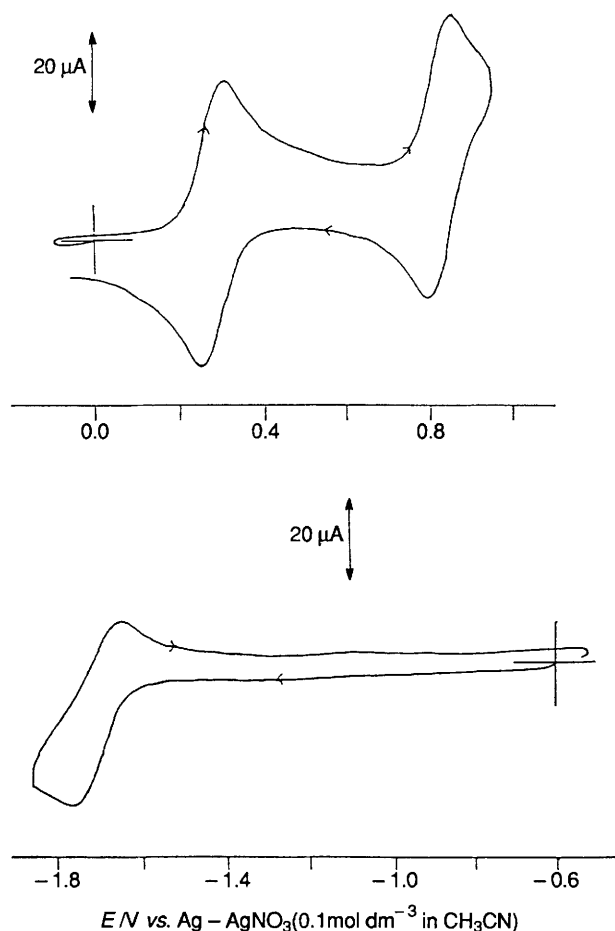
In complex **2** the terminal methyl group of the axial ethyl ligand is two-fold disordered about the crystallographic mirror plane. The H_2O –Co–Et fragment in the molecule is characterized by Co–C and Co–O bond lengths of 1.977(4) and 2.137(3) Å, and by C–Co–O and Co–C–C angles of 174.1(2) and 123.3(3)°, respectively. The Co–C bond length is 'normal' for an ethylcobalt(III) complex.^{3,15} The Co–OH₂ distance is also comparable to that in $[\text{CoL}^2(\text{Et})(\text{H}_2\text{O})]^{2+}$ [2.20(1) Å]³ and $[\text{CoL}^2(\text{Me})(\text{H}_2\text{O})]^{2+}$ (2.16 Å)¹⁶ but significantly longer than that in related $[\text{CoL}(\text{H}_2\text{O})_2]^{3+}$ complexes (1.91 Å).¹⁷ The long Co–O bond is consistent with a strong *trans* effect of the alkyl group.^{3,15a,16} The C–C bond length of 1.441(9) Å of the axial ethyl group is close to that found in other ethylcobalt(III) complexes.¹⁸ The Co–N(amide) bond, 1.875(2) Å, is significantly shorter than that to the pyridyl N atom, 1.975(2) Å, the former being comparable to Co–N(peptide) bonds, 1.87(1) Å.¹⁹

In both structures the amide ligand is approximately planar (maximum out-of-plane distance: 0.030 for **1**; 0.052 Å for **2**). The dihedral angle between the essentially planar 1,2-diaminobenzene unit and the pyridyl ring is less than 3°. So in contrast to $[\text{Cu}(\text{bpb})(\text{H}_2\text{O})]$ ²⁰ the steric repulsion which arises from the intramolecular non-bonding contact of H(9) and H(9') (1.95 for **1** and 1.93 Å for **2**) does not significantly alter the planarity of the amide ligand.

The co-ordinated water molecule forms hydrogen bonds with the carbonyl oxygen atoms in adjacent molecules to form a chain parallel to the *b* axis. Similar packings were found in

Table 4 Selected bond distances (Å) and angles (°) in [Co(bpc)(CH₂CH₂CMe=CH₂)(H₂O)] **1** and [Co(bpb)Et(H₂O)] **2** with e.s.d.s in parentheses

	Compound 1	Compound 2		Compound 1	Compound 2
Co–O(2)	2.136(5)	2.137(3)	C(2)–C(3)	1.393(6)	1.398(4)
Co–N(1)	1.877(4)	1.875(2)	C(3)–C(3') ^a	1.389(5)	1.402(4)
Co–N(2)	1.970(4)	1.975(2)	C(4)–C(5)	1.502(6)	1.500(3)
Co–C(10)	1.994(7)	1.977(4)	C(5)–C(6)	1.380(7)	1.383(4)
Cl–C(1)	1.750(5)		C(6)–C(7)	1.383(7)	1.379(4)
O(1)–C(4)	1.243(6)	1.243(3)	C(7)–C(8)	1.352(7)	1.360(4)
N(1)–C(3)	1.402(5)	1.410(4)	C(8)–C(9)	1.373(7)	1.368(5)
N(1)–C(4)	1.321(6)	1.335(3)	C(10)–C(11)	1.47(2)	1.441(9)
N(2)–C(5)	1.353(6)	1.349(3)	C(11)–C(12)	1.52(1)	
N(2)–C(9)	1.342(6)	1.333(4)	C(12)–C(13)	1.34(1)	
C(1)–C(1') ^a	1.350(5)	1.379(3)	C(12)–C(14)	1.52(2)	
C(1)–C(2)	1.384(7)	1.398(4)	O(1)···O(2) ^b	2.833(4)	2.791(3)
O(2)–Co–N(1)	90.5(1)	90.56(8)	N(1)–Co–N(1') ^a	84.8(1)	84.65(7)
O(2)–Co–N(2)	88.2(1)	87.94(8)	N(1)–Co–N(2') ^a	167.5(1)	167.39(6)
O(2)–Co–C(10)	180.1(8)	174.1(2)	N(2)–Co–C(10)	91.8(1)	88.6(1)
N(1)–Co–N(2)	82.8(2)	82.87(8)	N(2)–Co–N(2') ^a	109.5(1)	109.58(7)
N(1)–Co–C(10)	89.8(2)	93.8(1)			

Symmetry codes: ^a $x, \frac{1}{2} - y, z$; ^b $1 - x, 1 - y, 1 - z$.**Fig. 6** Cyclic voltammogram of [Co(bpb)Me(H₂O)] in MeCN (0.1 mol dm⁻³ NBu₄BF₄) (working electrode, glassy carbon disc; scan rate, 100 mV s⁻¹)

both structures. Fig. 5 illustrates the hydrogen-bonding scheme in **1**.

Electrochemistry.—The cyclic voltammogram of [Co(bpb)Me(H₂O)] in acetonitrile exhibits two reversible oxidation couples at +0.22 and +0.77 V vs. ferrocenium–ferrocene and a quasi-reversible reduction couple with a low i_p/i_{p_a} value at $E_{pc} = -1.81$ V (Fig. 6). Controlled-potential coulometry at +0.30 V vs. Ag–AgNO₃ (0.1 mol dm⁻³ in MeCN) showed that

Table 5 Summary of cyclic voltammetric data for the oxidation of 0.973 mmol dm⁻³ of [Co(bpb)Me(H₂O)] to [Co(bpb)Me(H₂O)]⁺ in acetonitrile with 0.1 mol dm⁻³ tetrabutylammonium tetrafluoroborate as supporting electrolyte (working electrode: glassy carbon disc, area = 0.22 cm²)

Scan rate, v/mV s ⁻¹	Current ratio i_p/i_{p_a}	Current function $i_p v^{-1}/mA s^{\frac{1}{2}} V^{-\frac{1}{2}}$
200	1.00	0.203
100	0.98	0.202
50	0.96	0.201
20	0.89	0.205
10	0.82	0.210
5	0.77	0.212

$n = 1.02$, establishing a one-electron oxidative process for the first oxidation couple. The one-electron oxidized product has been characterized by ultraviolet–visible spectroscopy. Magnetic susceptibility measurement (Evans method) revealed a μ_{eff} of 1.83, characteristic of the spin-only value of one unpaired electron. During oxidation, the peaks at 266, 342 and 425 nm decreased in intensity while a peak at 324 nm and a featureless broad band in the 600–900 nm region appeared. Isosbestic points were observed at 280, 330 and 378 nm, showing that the oxidation was clean (Fig. 7). The one-electron oxidation is reversible and occurs without secondary chemical reactions as the original electronic absorption spectrum can be regenerated upon electrochemical reduction of the oxidized product. However, after storing the one-electron oxidized product in the dark for 16 h at room temperature it is found partially to decompose.

Results of the scan-rate dependence of the first oxidation couple are in Table 5. Between scan rates of 200 and 5 mV s⁻¹ the peak-to-peak separation, ΔE_p (60–65 mV), and the current function, $i_p/v^{\frac{1}{2}}$, are relatively independent of the scan rate, v , typical of diffusion-controlled experiments with fast simple one-electron transfer at the electrode without a preceding chemical reaction step. This is further supported by the observation of a linear Levich plot in rotating-disc voltammetric studies with a calculated diffusion coefficient of 12.9×10^{-3} cm² s⁻¹. A calculated n value of 1 has also been obtained from the combined results of linear-sweep and rotating-disc voltammetry, which agrees well with that obtained by controlled-potential coulometry. However, the current ratio, i_p/i_{p_a} , of the first oxidation couple is found to decrease from 1.00 at a scan rate of 200 mV s⁻¹ to 0.77 at 5 mV s⁻¹, indicating a slow chemical reaction occurs after the electron transfer. For the second

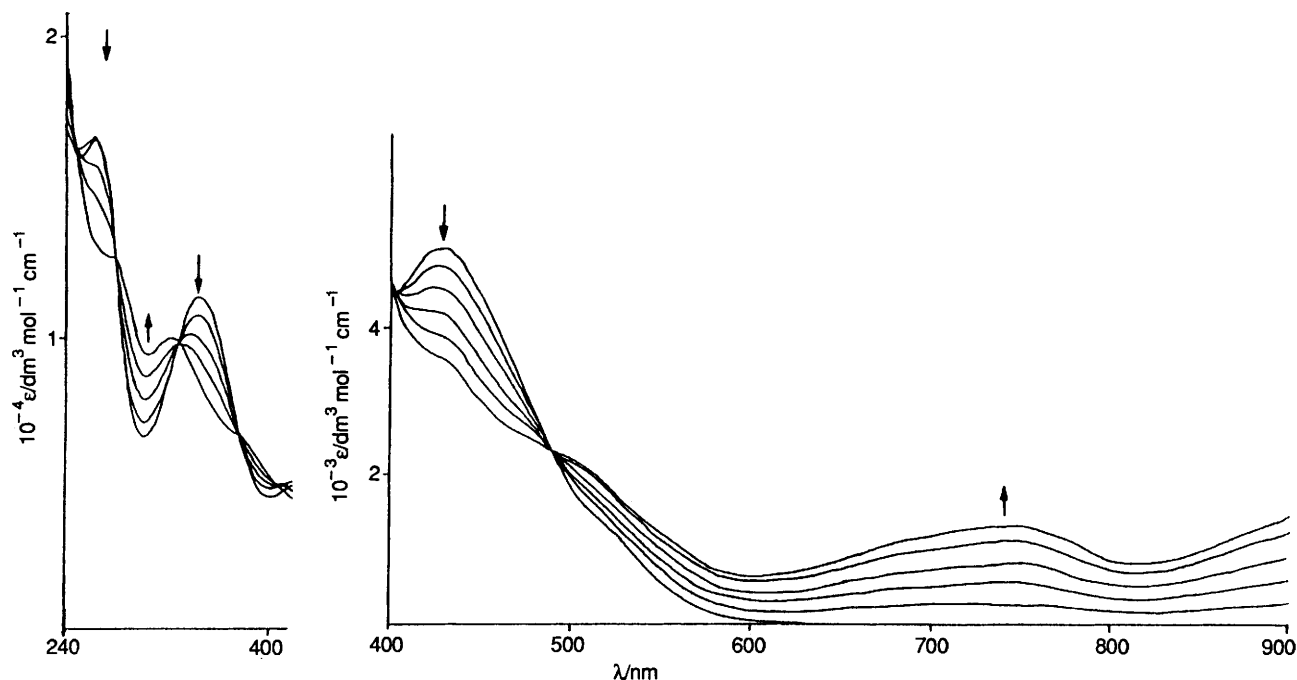


Fig. 7 Ultraviolet-visible spectral changes of $[\text{Co}(\text{bpb})\text{Me}(\text{H}_2\text{O})]$ in acetonitrile ($0.1 \text{ mol dm}^{-3} \text{ NBu}_4\text{BF}_4$) during controlled-potential electrolysis at $+0.50 \text{ V}$ vs. $\text{Ag}-\text{AgNO}_3$ (0.1 mol dm^{-3} in MeCN)

Table 6 Cyclic voltammetric data for some cobalt complexes of bpb and bpc ligands in (a) acetonitrile and (b) methanol ($0.1 \text{ mol dm}^{-3} \text{ NBu}_4\text{BF}_4$; working electrode, glassy carbon; scan rate, 100 mV s^{-1})

(a) In acetonitrile

Compound	First oxidation		Second oxidation	First reduction	
	E° (E_{p_a})	i_{p_c}/i_{p_a}	E° (E_{p_s})	E_{p_c}	$i_{p_c}/i_{p_{ox}}^b$ (n) ^c
$[\text{Co}(\text{bpb})\text{Me}(\text{H}_2\text{O})]$	+0.22	0.98	+0.77	-1.81	0.86
$[\text{Co}(\text{bpb})\text{Et}(\text{H}_2\text{O})]$	+0.18	1.00	(+0.75)	-1.96	1.02
$[\text{Co}(\text{bpb})(\text{CH}_2\text{CH}_2\text{CMe}=\text{CH}_2)(\text{H}_2\text{O})]$	+0.21	0.98	+0.52	-1.89	0.96
$[\text{Co}(\text{bpb})\text{Pr}^i(\text{H}_2\text{O})]$	(+0.19)	—	(+0.71)	-1.95	0.90
$[\text{Co}(\text{bpb})(\text{py})_2]\text{ClO}_4^d$	+0.75	0.80	(+1.20)	-0.62	0.53 (0.98)
$[\text{NBu}_4][\text{Co}(\text{bpb})(\text{CN})_2]$	+0.40	1.00	(+0.99)	-1.88	0.79
$\text{Na}[\text{Co}(\text{bpb})(\text{N}_3)_2]^e$	+0.34	0.72	—	-1.27	0.58
$[\text{Co}(\text{bpc})(\text{py})_2]\text{ClO}_4$	+0.91	0.80	+1.40	-0.53	0.62
$\text{Na}[\text{Co}(\text{bpc})(\text{N}_3)_2]$	+0.51	0.94	+0.97	-1.11	0.70

(b) In methanol

Compound	Oxidation		Reduction	
	E° (E_{p_a})	i_{p_c}/i_{p_a}	E_{p_c}	$i_{p_c}/i_{p_{ox}}^b$
$[\text{Co}(\text{bpb})\text{Me}(\text{H}_2\text{O})]$	+0.30	0.95	-1.82	1.96
$[\text{Co}(\text{bpb})(\text{CH}_2\text{CH}_2\text{CMe}=\text{CH}_2)(\text{H}_2\text{O})]$	+0.30	0.98	-1.90	2.08
$\text{Na}[\text{Co}(\text{bpb})(\text{CN})_2]$	+0.48	1.00	-1.51	0.84
$[\text{Co}(\text{bpc})\text{Me}(\text{H}_2\text{O})]$	+0.45	1.02	-1.72	1.92
$[\text{Co}(\text{bpc})(\text{CH}_2\text{CH}_2\text{CMe}=\text{CH}_2)(\text{H}_2\text{O})]$	(+0.50)	—	-1.85	1.74
$\text{Na}[\text{Co}(\text{bpc})(\text{CN})_2]$	+0.65	0.95	-1.42	0.69
$\text{Na}[\text{Co}(\text{bpc})(\text{N}_3)_2]$	+0.57	0.80	-0.84	0.71

^a E° in V vs. ferrocenium-ferrocene is reported for reversible couples, E_{p_a} and E_{p_c} for irreversible couples. ^b i_{p_c} and $i_{p_{ox}}$ are the peak currents for the reduction and the first oxidation couple respectively. ^c The number of electrons counted by controlled-potential coulometry. ^d Second reduction: $E^\circ = -1.68 \text{ V}$, $i_{p_c}/i_{p_{ox}} = 0.72$ ($n = 1.85$). ^e Second reduction: $E^\circ = -1.74 \text{ V}$, $i_{p_c}/i_{p_{ox}} = 0.82$.

oxidation couple a linear Levich plot is also obtained. A slope ratio of 1.15:1 between the Levich plots for the two oxidation couples established the one-electron transfer nature of the second oxidation couple. Determination of the value of n for the second oxidation couple by controlled-potential coulometry was unsuccessful since the current did not drop to zero even after 4 electrons mol^{-1} had been passed. This is probably a result of the high instability and/or oxidizing power of the two-electron oxidized product.

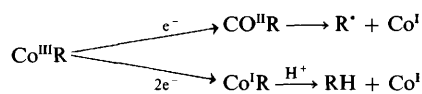
Cyclic voltammetric data for other cobalt complexes are summarized in Table 6. For the $[\text{Co}(\text{bpb})\text{R}(\text{H}_2\text{O})]$ complexes ($\text{R} = \text{Et}$, Pr^i or $\text{CH}_2\text{CH}_2\text{CMe}=\text{CH}_2$) the first oxidation couples have virtually identical formal potentials to that of $[\text{Co}(\text{bpb})\text{Me}(\text{H}_2\text{O})]$. This is in contrast to the $\text{Co}^{\text{III}}-\text{Co}^{\text{IV}}$ couples of $[\text{Co}(\text{salen})\text{R}(\text{py})]$ [$\text{salen} = \text{ethylenebis}(\text{salicylideneimine})$; $\text{R} = \text{Me}$, Et , Pr^i , Pr^n or Bu^n]²¹ where the E_1 values were spread over a range of 0.25 V. Thus, the first oxidation couple of $[\text{Co}(\text{bpb})\text{R}(\text{H}_2\text{O})]$ is suggested to be mainly ligand-centred.

This is also supported by the fact that the E° of $[\text{Rh}(\text{bpb})\text{R}(\text{H}_2\text{O})]^{2+}$ and their cobalt analogues are very similar.

The cyclic voltammetric results show that not all the first oxidation couples of non-organo complexes of $\text{Co}(\text{bpb})$ are reversible. The stability of the one-electron oxidized product varies to different extents as reflected by the current ratio, i_p/i_{p_1} . At a scan rate of 100 mV s^{-1} , i_p/i_{p_1} decreases in the series $[\text{Co}(\text{bpb})(\text{CN})_2]^- > [\text{Co}(\text{bpb})(\text{py})_2]^+ > [\text{Co}(\text{bpb})(\text{N}_3)_2]^-$. Only $[\text{Co}(\text{bpb})(\text{CN})_2]^-$ has a stability towards oxidation comparable to that of $[\text{Co}(\text{bpb})\text{Me}(\text{H}_2\text{O})]$. The increase in E° parallels the increase in the charge on the metal complex. For complexes bearing the same charge the difference in E° is small. This indicates the dominance of the potential-energy terms in charging the complexes over the effect of donor strength of the axial ligands. The high donor strength of the alkyl ligand is reflected in the exceptionally low E° value. Accordingly, it is plausible to postulate that the one-electron oxidation reaction is mainly ligand-centred with a small degree of metal character.

The reduction potential of the non-organocobalt complexes again correlates with the charge of the complexes, with the positively charged complexes being reduced at more anodic potentials. In contrast to the oxidation process, the axial ligands have a profound effect on the E_{p_c} value of the reduction process. Thus, it is suggested that the reduction processes are metal-centred. The reduction waves of the non-organocobalt complexes, assignable to the $\text{Co}^{\text{III}}-\text{Co}^{\text{II}}$ couple, are extended with low $i_{p_c}/i_{p_{ox}}$ values, indicating a slow heterogeneous electron transfer commonly found for cobalt complexes.

Similarly, the cyclic voltammograms of the organocobalt complexes exhibit irreversible reduction couples. The reduction processes are solvent dependent as reflected by their current ratios. Controlled-potential coulometric experiments established that one-electron reduction occurs in acetonitrile whereas two-electron reduction occurs in methanol. Similar results are observable for other organocobalt complexes of salen and acen ligands^{2,23} [acen = ethylenebis(acetylacetonimine)]. In aprotic solvents, homolytic cleavage of metal-carbon bonds occurs while in protic solvents, such as methanol, decomposition involving electrophilic attack at the α -carbon is possible (Scheme 2).



Scheme 2

Due to the insolubility of the $[\text{Co}(\text{bpc})\text{R}(\text{H}_2\text{O})]$ complexes in acetonitrile, the cyclic voltammograms were recorded in methanol. The redox pattern resembles that of the $\text{Co}(\text{bpb})$ complexes. However, fewer couples were observed due to the thinner potential screening window of methanol. The first oxidation couples of the $\text{Co}(\text{bpc})$ complexes are shifted 0.12–0.17 V to anodic potentials relative to the corresponding $\text{Co}(\text{bpb})$ complexes. This further suggests that the oxidation is essentially ligand-centred.

Acknowledgements

We acknowledge support from the University of Hong Kong and the University and Polytechnic Grants Committee.

References

- 1 *Modern Synthetic Methods*, ed. R. Scheffold, Wiley, New York, 1983, vol. 3, pp. 355–440.
- 2 K. Kanamori, W. E. Broderick, R. F. Jordan, R. D. Willett and J. I. Legg, *J. Am. Chem. Soc.*, 1986, **108**, 7122.
- 3 A. Bakac and J. H. Espenson, *Inorg. Chem.*, 1987, **26**, 4353.
- 4 C. M. Che and W. K. Cheng, *J. Chem. Soc., Chem. Commun.*, 1986, 1443.
- 5 C. M. Che, W. K. Cheng and T. C. W. Mak, *J. Chem. Soc., Chem. Commun.*, 1986, 200.
- 6 D. J. Barnes, R. L. Chapman, R. S. Vagg and E. C. Watton, *J. Chem. Eng. Data*, 1978, **23**, 349.
- 7 R. L. Chapman and R. S. Vagg, *Inorg. Chim. Acta*, 1979, **33**, 227.
- 8 C. M. Che, K. Y. Wong and F. C. Anson, *J. Electroanal. Chem.*, 1987, **226**, 211.
- 9 P. Main, S. J. Fiske, S. E. Hull, L. Lessinger, G. Germain, J. P. Declercq and M. M. Woolfson, MULTAN 82, A System of Computer Programs for the Automatic Solution of Crystal Structures, Universities of York and Louvain, 1982.
- 10 SDP, Enraf-Nonius Structure Determination Package, Enraf-Nonius, Delft, 1985.
- 11 *International Tables for X-Ray Crystallography*, Kynoch Press, Birmingham, 1974, vol. 4, pp. 99–149.
- 12 K. Nakamoto, *IR Spectra of Inorganic and Coordination Compounds*, Wiley, New York, 1963.
- 13 J. M. Pratt and P. J. Craig, *Adv. Organomet. Chem.*, 1973, **11**, 332; C. Floriani, M. Puppis and F. Calderazzo, *J. Organomet. Chem.*, 1968, **12**, 209; G. N. Schrauzer, J. W. Sibert and R. J. Windgassen, *J. Am. Chem. Soc.*, 1968, **90**, 2441; D. A. Clarke, D. Dolphin, R. Grigg, A. W. Johnson and H. A. Pinnock, *J. Chem. Soc. C*, 1968, 881; G. Costa, G. Mestroni and E. de Savorgnani, *Inorg. Chim. Acta*, 1969, **3**, 323.
- 14 (a) F. C. Anson, T. J. Collins, R. J. Coots, S. L. Gipson and T. G. Richmond, *J. Am. Chem. Soc.*, 1984, **106**, 5037; (b) T. J. Collins, T. G. Richmond, B. D. Santarsiero and B. G. R. T. Treco, *J. Am. Chem. Soc.*, 1986, **108**, 2088.
- 15 (a) P. J. Toscano and L. G. Marzilli, *Prog. Inorg. Chem.*, 1984, **31**, 105; (b) N. Bresciani-Pahor, L. Randaccio, E. Zangrando and P. J. Toscano, *Inorg. Chim. Acta*, 1985, **96**, 193; (c) L. McFadden and A. T. McPhail, *J. Chem. Soc., Dalton Trans.*, 1974, 363.
- 16 M. J. Hegg, J. F. Endicott and M. D. Glick, *Inorg. Chem.*, 1981, **20**, 1196.
- 17 J. F. Endicott, B. Durham, M. D. Glick, T. J. Anderson, J. M. Kuszaj, W. G. Schmonsees and K. P. Balakrishnan, *J. Am. Chem. Soc.*, 1981, **103**, 1431.
- 18 M. Calligaris, D. Minichelli, G. Nardin and L. Randaccio, *J. Chem. Soc. A*, 1971, 2720; A. L. Crumbliss, J. T. Bowman, P. L. Gaus and A. T. McPhail, *J. Chem. Soc., Chem. Commun.*, 1973, 415.
- 19 M. T. Barnet, H. C. Freeman, D. A. Buckingham, I. N. Hsu and D. van der Helm, *Chem. Commun.*, 1970, 367.
- 20 R. L. Chapman, F. S. Stephens and R. S. Vagg, *Inorg. Chim. Acta*, 1980, **43**, 29.
- 21 I. Y. Levitin, A. L. Sigan and M. E. Volphin, *J. Chem. Soc., Chem. Commun.*, 1975, 469.
- 22 S. T. Mak, V. W. W. Yam, C. M. Che and T. C. W. Mak, *J. Chem. Soc., Dalton Trans.*, 1990, 2555.
- 23 G. Costa, G. Mestroni, A. Puxeddu and C. Reisenhofer, *J. Chem. Soc. A*, 1970, 2870; G. Costa, *Coord. Chem. Rev.*, 1972, **8**, 63.

Received 17th January 1991; Paper 1/00256B